INL/EXT-14-**33257**

Light Water Reactor Sustainability Program

3D J-Integral Capability in Grizzly

September 2014

DOE Office of Nuclear Energy

INL/EXT-14-33257

Light Water Reactor Sustainability Program

3D J-Integral Capability in Grizzly

Benjamin Spencer[1], Marie Backman[2], Pritam Chakraborty[1], and William Hoffman[1]

[1]Idaho National Laboratory
[2]University of Tennessee

September 2014

Idaho National Laboratory
Idaho Falls, Idaho 83415

http://www.inl.gov/lwrs

Prepared for the
U.S. Department of Energy
Office of Nuclear Energy
Under DOE Idaho Operations Office
Contract DE-AC07-05ID14517

Executive Summary

This report summarizes work done to develop a capability to evaluate fracture contour J-integrals in 3D in the Grizzly code. In the current fiscal year, a previously-developed 2D implementation of a J-integral evaluation capability has been extended to work in 3D, and to include terms due both to mechanically-induced strains and due to gradients in thermal strains. This capability has been verified against a benchmark solution on a model of a curved crack front in 3D. The thermal term in this integral has been verified against a benchmark problem with a thermal gradient.

These developments are part of a larger effort to develop Grizzly as a tool that can be used to predict the evolution of aging processes in nuclear power plant systems, structures, and components, and assess their capacity after being subjected to those aging processes.

The capabilities described here have been developed to enable evaluations of Mode-I stress intensity factors on axis-aligned flaws in reactor pressure vessels. These can be compared with the fracture toughness of the material to determine whether a pre-existing flaw would begin to propagate during a postulated pressurized thermal shock accident. This report includes a demonstration calculation to show how Grizzly is used to perform a deterministic assessment of such a flaw propagation in a degraded reactor pressure vessel under pressurized thermal shock conditions. The stress intensity is calculated from J, and the toughness is computed using the fracture master curve and the degraded ductile to brittle transition temperature.

CONTENTS

FIGURES

TABLES

ACRONYMS

EONY	Eason, Odette, Nanstad, and Yamamoto
LEFM	Linear elastic fracture mechanics
LWR	Light water reactor
PTS	Pressurized Thermal Shock
RPV	Reactor Pressure Vessel

1 3D J-Integral Implementation

Linear elastic fracture mechanics (LEFM) is widely accepted as an appropriate methodology to assess the susceptibility of a reactor pressure vessel (RPV) to fracture during a loading event [3]. LEFM is based on the assumption that the material ahead of a crack front behaves in a linearly elastic manner, resulting in a singularity in the stress field ahead of the crack tip. The mode-I stress intensity factor, K_I is a measure of the degree of the singularity of that field on a crack under mode-I (normal to crack plane) loading.

A finite element calculation in which a crack is represented in the mesh geometry can be used to calculate the displacement and stress fields in the vicinity of the crack. One straightforward way to evaluate the stress intensity from a finite element solution is through the J-integral [4], which provides the mechanical energy release rate. If the crack is subjected to pure mode-I loading, K_I can be calculated from J using the following relationship:

$$J = \begin{cases} \dfrac{1-\nu^2}{E} K_I^2 & \text{plane strain} \\ \dfrac{1}{E} K_I^2 & \text{plane stress} \end{cases} \tag{1}$$

where E is the Young's modulus and ν is the Poisson's ratio. For assessing flaws in a RPV, plane strain conditions are assumed.

The J-integral was originally formulated as an integral over a closed curve around the crack tip in 2D. It can alternatively be expressed as an integral over a surface in 2D or a volume in 3D using the method of [5], which is more convenient for implementation within a finite element code. As described in [6], during the previous fiscal year, a capability to evaluate the J-integral in Grizzly was developed based on this method.

Following the terminology of [7], the integrated value of the J-integral over a segment of a crack front, represented as $\bar{J}$, can be expressed as a summation of four terms:

$$\bar{J} = \bar{J}_1 + \bar{J}_2 + \bar{J}_3 + \bar{J}_4 \tag{2}$$

where the individual terms are defined as:

$$\bar{J}_1 = \int_{V_0} \left(P_{ji} \frac{\partial u_i}{\partial X_k} \frac{\partial q_k}{\partial X_j} - W \frac{\partial q_k}{\partial X_k} \right) dV_0 \tag{3}$$

$$\bar{J}_2 = -\int_{V_0} \left(\frac{\partial W}{\partial X_k} - P_{ji} \frac{\partial^2 u_i}{\partial X_j \partial X_k} \right) q_k dV_0 \tag{4}$$

$$\bar{J}_3 = -\int_{V_0} \left(T \frac{\partial q_k}{\partial X_k} - \rho \frac{\partial^2 u_i}{\partial t^2} \frac{\partial u_i}{\partial X_k} q_k + \rho \frac{\partial u_i}{\partial t} \frac{\partial^2 u_i}{\partial t \partial X_k} q_k \right) dV_0 \tag{5}$$

$$\bar{J}_4 = -\int_{A_0} t_i \frac{\partial u_i}{\partial X_k} q_k dA_0 \tag{6}$$

In these equations, V_0 is the undeformed volume, A_0 is the combined area of the two crack faces, P_{ji} is the 1st Piola-Kirchoff stress tensor, u_i is the displacement vector, X_k is the undeformed coordinate vector, W is the stress-work density, T is the kinetic energy density, t is time, ρ is the material density, and t_i is the vector of tractions applied to the crack face.

The vector field q_k is a vector field that is oriented in the crack normal direction. This field has a magnitude of 1 between the crack tip and the inner radius of the ring over which the integral is to be performed, and drops from 1 to 0 between the inner and outer radius of that ring, and has a value of 0 elsewhere. In 3D, J is evaluated by calculating the integral $\bar{J}$ over a segment of the crack front. A separate q field is formed for each segment along the crack front, and for each ring over which the integral is to be evaluated. Each of

those q fields is multiplied by a weighting function that varies from a value of 0 at the ends to a finite value in the middle of the segment. The value of J at each point on the curve is evaluated by dividing $\bar{J}$ by the integrated value of the weighting function over the segment containing that point.

The first term in $\bar{J}$, $\bar{J}_1$, represents the effects of strain energy in homogeneous material in the absence of thermal strains or inertial effects. The second term, $\bar{J}_2$, accounts for the effects of material inhomogenieties and gradients of thermal strain. For small strains, this term can be represented as:

$$\bar{J}_2 = \int_{V_0} \sigma_{ij} \left[\alpha_{ij} \frac{\partial \bar{\theta}}{\partial X_k} + \frac{\partial \alpha_{ij}}{\partial X_k} \bar{\theta} \right] q_k dV_0 \tag{7}$$

where σ_{ij}, α_{ij}, $\bar{\theta}$ and q_k are the Cauchy stress, thermal conductivity, and difference between the current temperature and a reference temperature, respectively.

The third term in $\bar{J}$, $\bar{J}_3$, accounts for inertial effects in a dynamic analysis, and the fourth term, $\bar{J}_4$ accounts for the effects of surface tractions on the crack face.

The implementation of the J-integral calculator in Grizzly can be used for arbitrary curved 3D crack fronts, and includes the $\bar{J}_1$ and $\bar{J}_2$ terms to account for the effects of quasistatic mechanically and thermally induced strains. The last two terms have not been implemented. Because the RPV analyses are all quasistatic, there are no inertial effects, so $\bar{J}_3 = 0$. $\bar{J}_4$ would be nonzero for surface-breaking cracks because of the effects of the fluid pressure, but its contribution is expected to be negligible relative to that of the first two terms.

To use the J-integral capability in Grizzly, a user specifies a set of nodes along the crack front, information used to calculate the crack normal directions along the crack front, and the inner and outer radii of the set of rings over which the integral is to be performed. Grizzly automatically defines the full set of q functions for each point along the crack front, and outputs either the value of J or K_I at each of those points. In addition, the user can ask for any other variable in the model to be output at points corresponding to those where J is evaluated along the crack front.

2 Verification Problems

The 3D J-integral evaluation capability in Grizzly has been verified against known analytical solutions. Comparisons with benchmark solutions for two problems are shown here.

2.1 3D curved crack front

Grizzly's 3D J-integral capability was verified against a solution for a semi-elliptic surface-breaking flaw in an elastic half space subjected to pure mode-I tensile loading published by Raju and Newman [8]. The finite element model used to represent this problem in Grizzly is shown in Figure 1a. This is a quarter-symmetry model. A symmetry plane on the left hand surface of the model passes through the middle of the crack, and is represented with appropriate zero displacement boundary conditions in the direction normal to that plane. A second symmetry plane passes through the bottom surface of the model, which is also the plane that the crack lies on. The plane on the right hand surface of the model is a free surface. The size of the model was selected to be sufficiently large to minimize edge effects. It has outer dimensions of 5m x 5m x 5m. The major and minor radii of the elliptical crack are 635mm and 254mm. Figure 1b shows a zoomed-in view of the mesh of the crack tip, which is meshed with a rounded tip with a radius of 1mm. The material is linearly elastic, with E=206.8 GPa and ν=0.3. J-integrals were evaluated using three contours having inner radii of 12.5mm, 25.0mm, and 37.5mm, and corresponding outer radii of 25.0mm, 37.5mm, and 50.0mm. Figure 1c shows the q function corresponding to the point where the crack tip intersects the free surface.

Figure 2 shows a plot of the values of J computed along the crack tip by Grizzly compared with the benchmark solution. These values are plotted as a function of the position along the crack front, measured by the angle. These computed values are in good agreement with the benchmark solution along the crack path. Results are shown here for one contour, but all contours produced very similar results.

2.2 Nonuniform thermal strain

The thermo-mechanical problem provided in [1] is used to verify the thermal term in the J-integral implementation. A schematic of the cracked geometry, boundary conditions and temperature distribution is shown in Fig. 3.

The following material properties: E = 207 GPa, $\nu = 0.3$, $\alpha = 1.35e^{-5}$, are used and a θ_e=10^oC is applied to perform plane strain thermo-mechanical simulation. The distribution of the stress ($\sigma_y y$) in the cracked geometry is shown in Fig. 4b. J-integral calculations are made on 4 different rings from the crack tip with a inner radius varying from 60-120 mm and thickness of 20 mm. The variation of q in the outermost ring is shown in Fig. 4a. A converged J value of 1.4056 MPa-mm is obtained which is compared to the analytical solution provided in [2] and is shown in Table 1.

Table 1: Comparison of J-integral values with analytical solution of 1.40615 MPa-mm obtained from [2] for thermo-mechanical problem.

Contour	Inner Radius	Outer Radius	J (MPa-mm)	% Difference
1	60	80	1.40565	0.036
2	80	100	1.4057	0.032
3	100	120	1.40577	0.028
4	120	140	1.40585	0.022

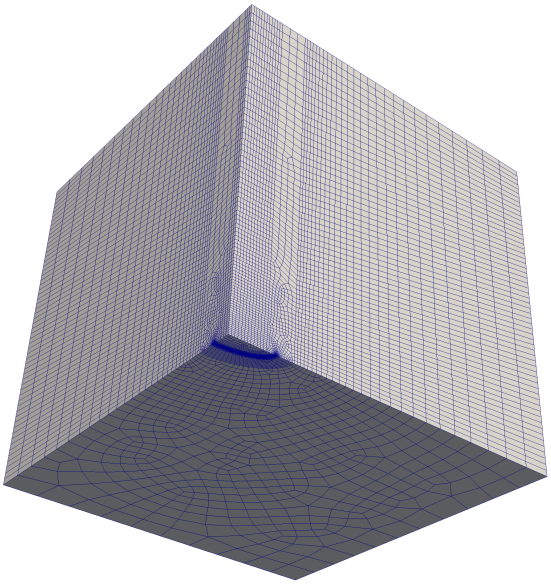

(a) Overview of model showing meshed curved elliptical crack

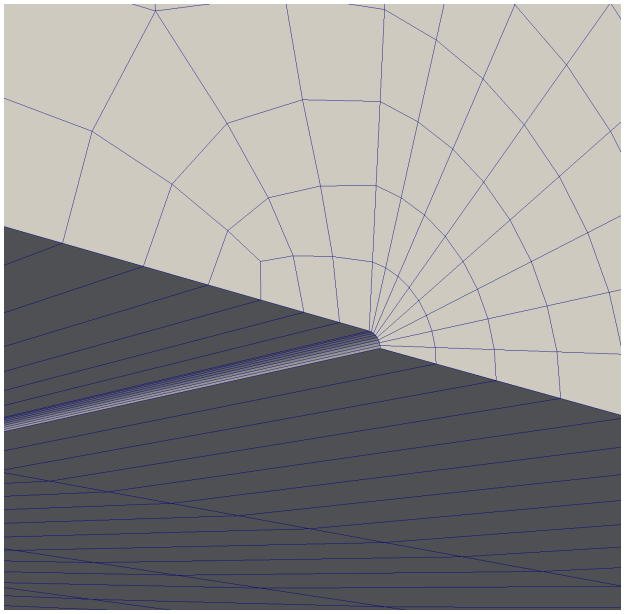

(b) Zoomed-in view of crack tip showing finite tip radius

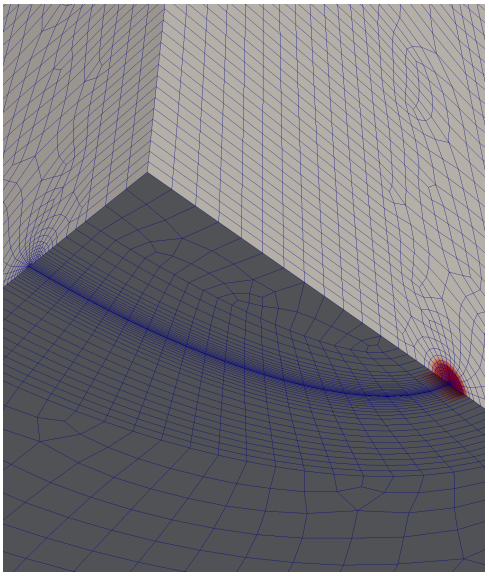

(c) View of curved crack front showing q function for node on crack front adjacent to free surface. In this plot, a value of 1 is red, and a value of 0 is white

Figure 1: Verification model of elliptical surface-breaking flaw

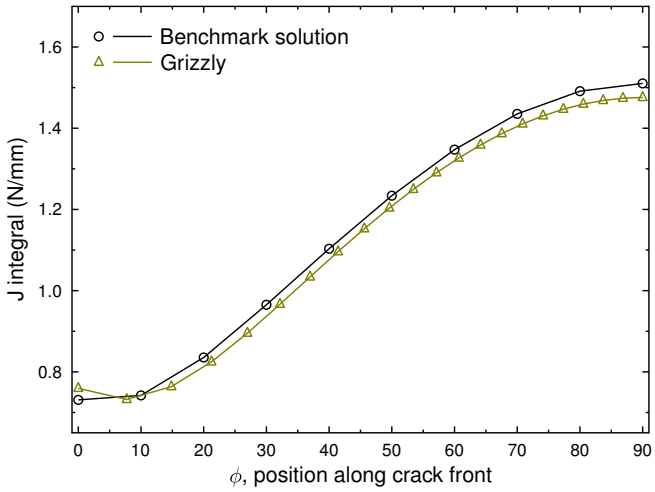

Figure 2: Grizzly-computed and benchmark solutions for J-integral as a function of position along crack front

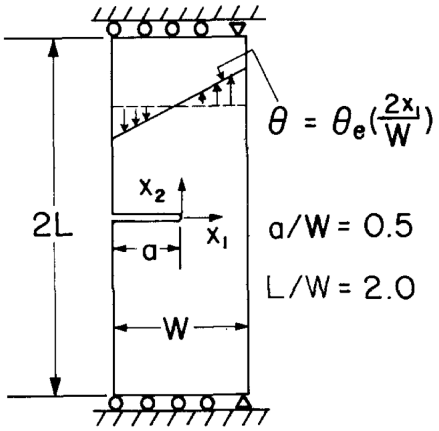

Figure 3: Schematic of crack geometry, boundary conditions and thermal load used in the thermo-mechanical verification problem (from [1]). a=252 mm, W = 504 mm, L = 1008 mm and θ_e=10oC is used.

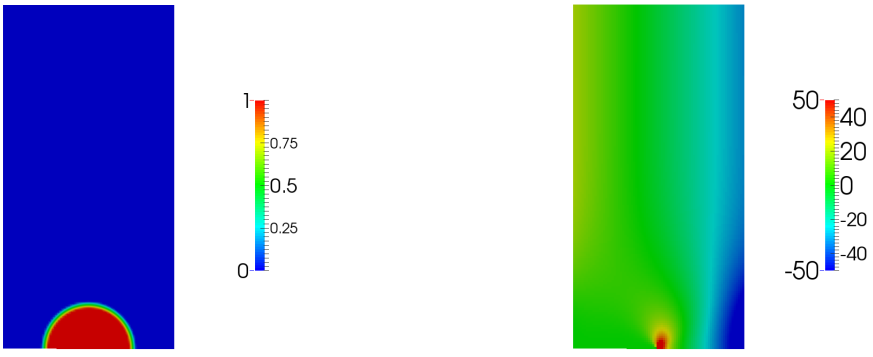

(a) Variation of q function in the outermost ring.

(b) Stress distribution (MPa).

Figure 4: Results from thermo-mechanical verification problem

3 Demonstration Application to Reactor Pressure Vessel

The 3D J-Integral evaluation capability in Grizzly can be used to perform a deterministic assessment of the susceptibility of a reactor pressure vessel (RPV) embrittled due to irradiation and thermal aging to fracture during a pressurized thermal shock (PTS) event. During a PTS scenario, there is a rapid drop in the temperature and pressure of the coolant in the RPV, which can cause strong temperature gradients through the wall of the vessel, and accompanying high tensile stresses in the interior of the vessel. In some scenarios, there can be a sudden repressurization of the vessel, further increasing the tensile stresses. The combination of high tensile stresses and lower temperatures, which put the steel in a state of decreased toughness, can potentially lead to crack propagation at the location of a pre-existing flaw.

Prior reports have detailed the development of capabilities in Grizzly to perform tightly coupled thermo-mechanical simulations of the global response of the RPV under such conditions, as well as of the spatial variation of embrittlement due to a given fluence distribution [9]. In that procedure, the embrittlement is calculated using the EONY model [10], and is represented in terms of the shift in the ductile to brittle transition temperature. More recently, a capability to embed a submodel representing the material in the vicinity of a flaw, represented geometrically as a feature of the finite element mesh, into the global model of the RPV has been demonstrated [11]. Temperature and displacement boundary conditions on the submodel are obtained from the response of the global model. The crack submodel can be embedded at arbitrary locations in the global model, and is subjected to the full loading history applied to the global model.

Two new capabilities developed in the current year have enabled the usage of these capabilities for a deterministic fracture assessment. The first of these is the ability to evaluate J-integrals along crack fronts in 3D. These domain integrals can now be performed on fracture submodels similar to those demonstrated previously, and used to calculate the mode-I stress intensity, K_I, as a function of position along the crack front and time.

The second capability used to enable fracture assessments is the ability to use the fracture master curve in conjunction with the transition temperature shift to calculate the mode-I fracture toughness, K_{IC} at the current temperature for each location in the model. The following equation describes K_{IC} calculated from the master curve for a given probability, P [12, 13]:

$$K_{IC} = K_{min} + \left[\ln\left(\frac{1}{1-P}\right)\right]^{0.25} \{31 - K_{min} + 77\exp[0.019(T - T_0)]\} \tag{8}$$

where K_{min} is the minimum fracture toughness, T is the current temperature, and T_0 is the ductile to brittle transition temperature, to which the shift calculated by the EONY model is applied. Because the temperature varies with time, this is computed at every time step. Grizzly's domain integral capability allows arbitrary variables to be output at positions along the crack front in conjunction with the output values of K_I, enabling direct comparisons of K_I and K_{IC} at each point along the crack at each time.

Prior demonstrations of the application of Grizzly to the thermomechanical analysis of an RPV were on a vessel without a liner. A new model for a generic, representative RPV has been developed that incorporates a stainless steel liner on the interior, as shown in Figure 5. In addition, a set of four submodels of the material in the vicinity of the flaw have been developed. These models represent axially and circumferentially oriented flaws. A variant of each of these was developed for an embedded flaw and a surface-breaking flaw, which passes through both the base material and the liner. Figure 5 shows the model of the axially-oriented, surface-breaking flaw. This report shows the results for this model, in which a semicircular flaw with a radius of 1cm penetrates through the liner, which has a thickness of 4.06mm, and into the base metal. The full set of models is shown in [14].

To demonstrate Grizzly's deterministic fracture assessment capability, this RPV model and submodel were subjected to a PTS transient event characterized by the coolant temperature and pressure histories shown in Figure 6. The analysis starts with the whole vessel at the initial coolant temperature, which is the normal

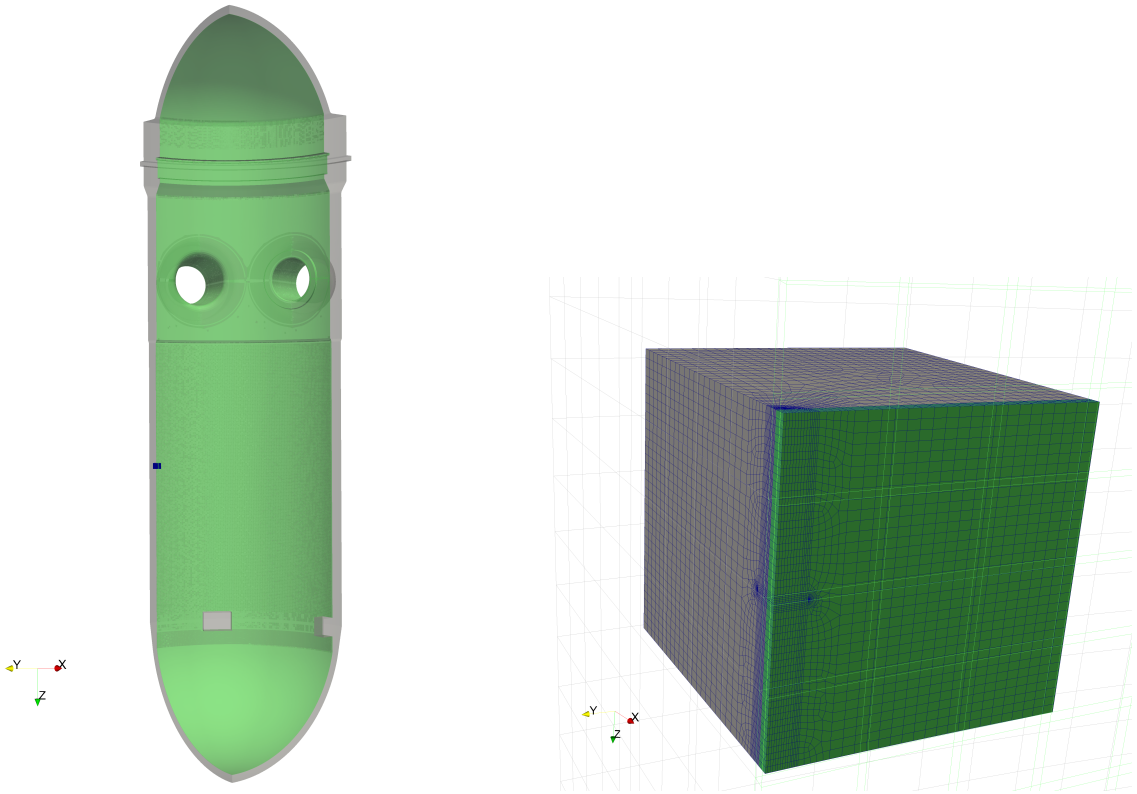

Figure 5: Overview (left) and detailed view (right) of global RPV model and submodel containing a semi-elliptic surface-breaking flaw with normal to the crack plane in the axial direction. The detailed view shows the mesh of the global model as a wireframe overlaid on the submodel mesh. The liner material is colored green in both views.

operating condition. The coolant temperature and pressure are then varied according to the functions shown. A heat transfer coefficient that also varies with time is used in conjunction with the coolant temperature to apply a thermal flux boundary condition.

Figure 7 shows the calculated mode-I stress intensity, K_I, as a function of the position along the crack front at various points in time during the PTS accident scenario. The position along the crack front is expressed in terms of the angle, ϕ, along the crack front. A point with $\phi = 0$ is on the outer face of the liner, and the deepest point on the crack is at $\phi = 90$. The effects of the liner are manifested as kinks in this plot. From this plot, it is evident that the highest stress intensity is at the deepest point in the crack.

Once the stress intensities are calculated, they can be compared with the toughness. Figure 8 shows the assumed fluence on the global model of the RPV, representative of the conditions after 32 years of operation, calculated using previously-developed procedures documented in [9]. This is used as input to the EONY model to calculate the transition temperature shift everywhere in the model, and that is in turn used as input into the fracture master curve to calculate the toughness at all positions along the crack front.

Figure 9 shows the history of the stress intensity at the deepest point in the crack compared with the toughness with 1% and 50% failure probabilities throughout the PTS event. The variation in both the stress intensity and the fracture toughness over time can clearly be seen in this plot. The toughness drops over time as the temperature at that point in the vessel drops. The stress intensity reaches a maximum early on in the analysis when the thermal gradient is the highest, but then drops as the temperature in the vessel equilibrates, reducing the thermal gradient and corresponding thermally-induced stresses. In this particular case, the loading is relatively low in comparison to the capacity, as it is well below the 1% probability

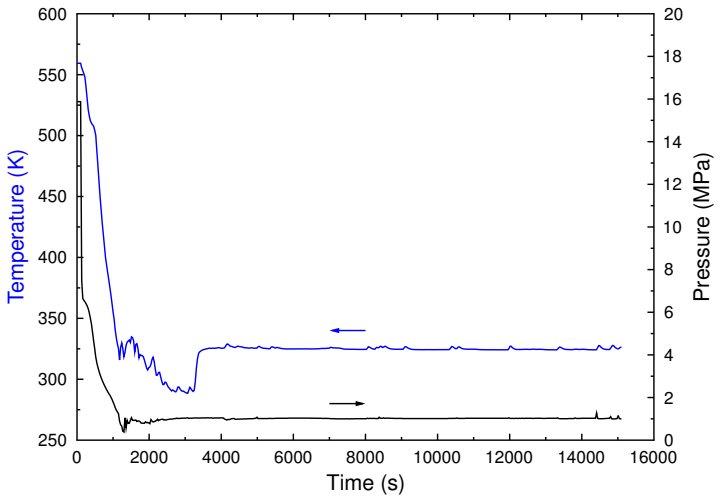

Figure 6: Temperature and pressure histories in a RPV for a PTS transient applied as boundary conditions at the inner surface of the full scale RPV model.

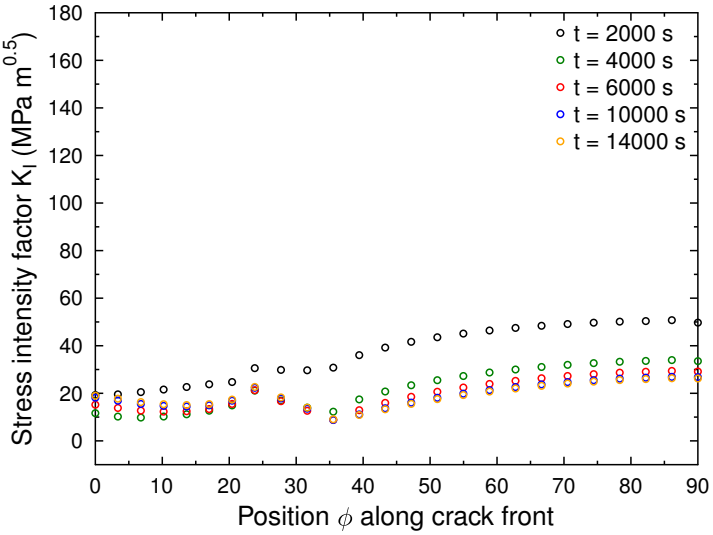

Figure 7: Stress intensity factor, K_I, as a function of position along crack front at various times during PTS transient.

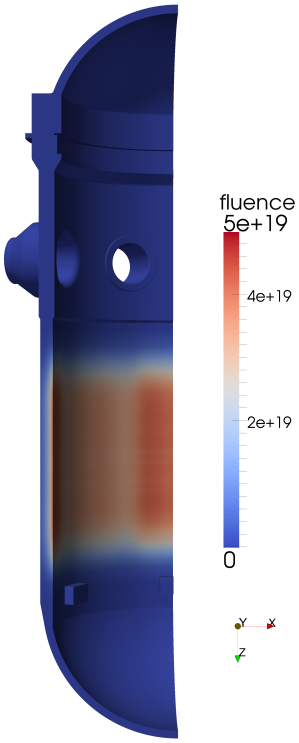

Figure 8: Distribution of accumulated neutron fluence in global RPV model after 32 years of operation.

toughness throughout the event. Other crack geometries and loading scenarios result in varying susceptibility to fracture. Results from analyses of a larger set of flaw geometries under more conditions are documented in [14].

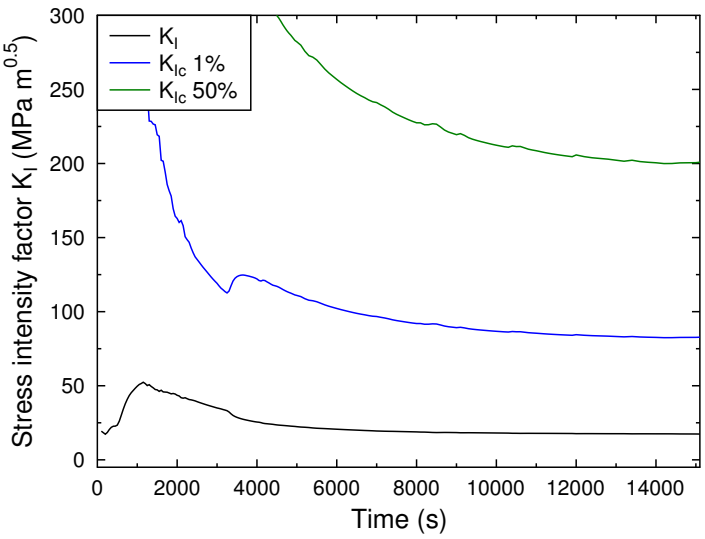

Figure 9: Stress intensity factor, K_I, compared with the fracture toughness, K_{IC} with failure probabilities of 1% and 50% for the PTS transient at the deepest point in the crack.

4 Summary

This report provides a summary and demonstration of new capabilities developed in Grizzly to permit a deterministic assessment of fracture in an embrittled RPV. The new capabilities developed during the current fiscal year that have enabled this simulation include enhancements to the J-integral capability and adding the ability to use the fracture master curve to evaluate the toughness at the current temperature. The J-integral capability has been expanded by enabling it to be evaluated on 3D models, including the term that accounts for gradients in thermal expansion, and adding the ability to output arbitrary variables along the crack front at points corresponding to those for which the J-integral is reported.

The combination of these new capabilities permits the evaluation and reporting of the mode-I stress intensity factor and the fracture toughness at each point along the crack front. These can be compared to assess the likelihood of crack propagation at every point along a postulated pre-existing flaw at each time step during a simulation of a PTS transient event. A new generic model of a RPV has been developed, together with submodels of flaws in various orientations. This report has demonstrated how Grizzly can be used on this model to calculate the global thermo-mechanical response, and output the history of the stress intensity and toughness at locations on a flaw.

5 References

1. C.F. Shih, B. Moran, and T. Nakamura. Energy release rate along a three-dimensional crack front in a thermally stressed body. *International Journal of Fracture*, 30:79–102, 1986.

2. I. W. Yu W. K. Wilson. The use of the j-integral in thermal stress crack problems. *International Journal of Fracture*, 15(4):377–387, 1979.

3. T. L. Dickson, P. T. Williams, and S. Yin. *Fracture Analysis of Vessels - Oak Ridge FAVOR, v09.1, Computer Code: User's Guide*. Oak Ridge National Laboratory, December 2009.

4. J. R. Rice. A path independent integral and the approximate analysis of strain concentration by notches and cracks. *Journal of Applied Mechanics*, 35(2):379, 1968.

5. F. Z. Li, C. F. Shih, and A. Needleman. A comparison of methods for calculating energy release rates. *Engineering Fracture Mechanics*, 21(2):405–421, 1985.

6. Stephen R. Novascone, Benjamin W. Spencer, and Jason D. Hales. Status report on the grizzly code enhancements. INL/EXT-13-30315, Idaho National Laboratory, Idaho Falls, ID, September 2013.

7. Brian Healy, Arne Gullerud, Kyle Koppenhoefer, Arun Roy, Sushovan RoyChowdhury, Matt Walters, Barron Bichon, Kristine Cochran, Adam Carlyle, James Sobotka, Mark Messner, and Robert Dodds. Warp3d-release 17.3.1. UILU-ENG-95-2012, University of Illinois at Urbana-Champaign, 2012.

8. I.S. Raju and J.C. Newman. Stress-intensity factors for a wide range of semi-elliptical surface cracks in finite-thickness plates. *Engineering Fracture Mechanics*, 11(4):817–829, January 1979.

9. Benjamin Spencer, Jeremy Busby, Richard Martineau, and Brian Wirth. A proof of concept: Grizzly, the LWRS program materials aging and degradation pathway main simulation tool. , Idaho National Laboratory, Idaho Falls, ID, 2012.

10. E.D. Eason, G.R. Odette, R.K. Nanstad, and T. Yamamoto. A physically-based correlation of irradiation-induced transition temperature shifts for RPV steels. *Journal of Nuclear Materials*, 433(1-3):240–254, February 2013.

11. Benjamin Spencer, Yongfeng Zhang, Pritam Chakraborty, S. Bulent Biner, Marie Backman, Brian Wirth, Stephen Novascone, and Jason Hales. Grizzly year-end progress report. INL/EXT-13-30316, Idaho National Laboratory, Idaho Falls, ID, September 2013.

12. K. Wallin. The scatter in K_{IC} results. *Engineering Fracture Mechanics*, 19(6):1085–1093, 1984.

13. ASTM. *Standard Test Method for Determination of Reference Temperature, To, for Ferritic Steels in Transition Range*, 13 edition, 2013.

14. Benjamin Spencer, Yongfeng Zhang, Pritam Chakraborty, Marie Backman, William Hoffman, Daniel Schwen, S. Bulent Biner, and Xianming Bai. Grizzly status report. INL/EXT-14-33251, Idaho National Laboratory, Idaho Falls, ID, September 2014.